

National Aeronautics and Space Administration
FINAL TECHNICAL REPORT FOR NAG 5-4112

Submitted to: Dr. Jean Swank, Code 662
NASA/Goddard Space Flight Center
Greenbelt, MD 20771

Submitted by: The Trustees of Columbia University
in the City of New York
351 Eng. Terrace
New York, New York 10027

Prepared by: Columbia Astrophysics Laboratory
Departments of Astronomy and Physics
Columbia University
550 West 120th Street, MC-5247
New York, New York 10027

Principal Investigator: Karen Leighly

Titles of Research: Variability & Spectral Studies of Luminous Seyfert 1
Galaxy Fairall 9

Search for the Reflection Component
in a Quasar: RXTE and ASCA Observations
of a Nearby Radio-Quiet Quasar MR 2251-178

Report Period: 15 April 1997 – 14 April 1998

July 1999

Final Report for NASA Grant NAG 5-4112 (XTE)
Variability & Spectral Studies of the Luminous Seyfert 1 Galaxy Fairall 9
Search for the Reflection Component in a Quasar –
RXTE and ASCA Observation of a Nearby Radio-Quiet Quasar MR 2251-178

K. M. Leighly

July 17 1999

ABSTRACT: Monitoring observations with interval of 3 days using *RXTE* of the luminous Seyfert 1 galaxy Fairall 9 were performed for one year. The purpose of the observations were to study the variability of Fairall 9 and compare the results with those from the radio-loud object 3C 390.3. The data has been received and analysis is underway, using the new background model. An observation of the quasar MR 2251–178 was made in order to determine whether or not it has a reflection component. Older background models gave an unacceptable subtraction and analysis is underway using the new background model. The observation of NGC 6300 showed that the X-ray spectrum from this Seyfert 2 galaxy appears to be dominated by Compton reflection.

REPORT:

Improvements in Background Model, Response and Analysis Software for RXTE: Previous to 1998, the background model for the *RXTE* Proportional Counter Array (PCA) did not provide an acceptable subtraction for faint sources such as AGN. An intensive study of this problem was carried out at the *RXTE* Guest observer facility from April to October 1998. The result was the new L7 background model. This model uses a sum of count rates from 7 detectors which have adjacent anodes to predict the rate in the top and mid layers. Another ingredient is count rate in the HEXTE particle monitor which is used to estimate the radiation dosage from the South Atlantic Anomaly (SAA) and modeled with a 240 minute half-life. Essential to this model is the assumption that no flux from the object can be detected in the bottom layer at low energies. Thus this background model can only be applied to objects with count rates $< 40 \text{ counts s}^{-1}$. This background model performs the best when data taken during the 30 minute interval after emergence from SAA passage are discarded, and when data taken when electron rate housekeeping parameter electronm greater than 0.1 are discarded.

The response matrix has also been improved recently. Now, response matrices are constructed for each observation. This makes it possible to account for two time-dependent effects: the slow drift in gain of approximately 1% over two years, and a slowly increasing xenon fraction in the propane layer. Application of this new response improved the spectra, especially in the 10–20 keV range where the flux is low and there is a lot of structure in the background.

Another property that has recently been improved is a better estimation of the uncertainty associated with the background. Previously, the statistics of the background reflected the length of the observation. However, the background model is constructed from many background observations, the total length of which is very much longer than a single obser-

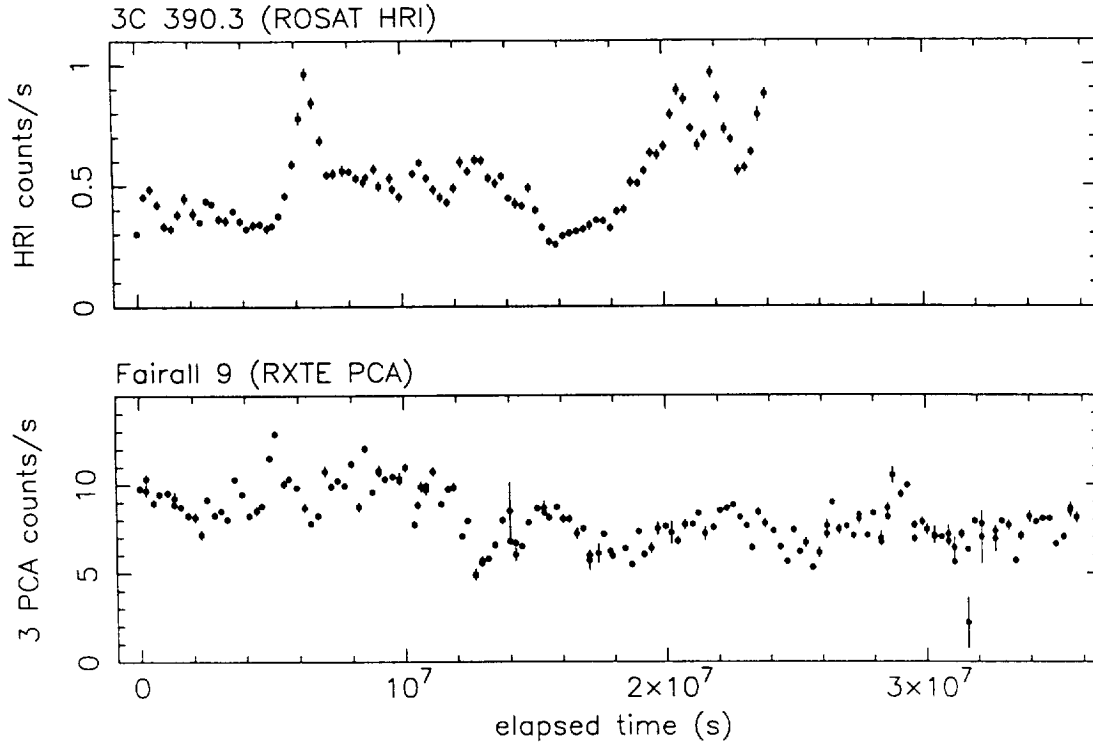


Figure 1: Light curves from the ROSAT monitoring of 3C 390.3 (top) and RXTE monitoring of Fairall 9 (bottom).

variation. Therefore, the uncertainties in the background spectra should be reduced to reflect this fact. A script to correct the background spectra was developed.

An improvement to the data analysis software has also recently been made with the addition of the *REX* script. This script permits analysis of a large number of observations to be done in a nearly automatic, hands-off manor. The use of this script permits analysis of AGN monitoring observations to be done quickly and easily.

Fairall 9: In 1995, we obtained the first well sampled AGN X-ray light curve on time scales from days to months from a ROSAT HRI monitoring campaign on 3C 390.3. The resulting light curve shows flares and quiescent periods indicative of nonlinear variability, and challenges current AGN X-ray variability models. However, 3C 390.3 has a compact radio jet which could be the origin of the X-ray emission (although there is also evidence the emission is isotropic) so the nonlinear variability observed may not be characteristic of AGN in general. To test this, we proposed RXTE snapshot observations every three days for 1 year of Fairall-9, which has similar X-ray luminosity and variability time scale as 3C 390.3, but is radio quiet. Our analysis plans also include using the total RXTE spectrum combined with archival ASCA spectra to determine whether the huge equivalent width (500-700eV) iron line observed in the ASCA spectrum originates from geometry, abundance or ionization factors.

The paper reporting the results is in preparation. The analysis is being performed by

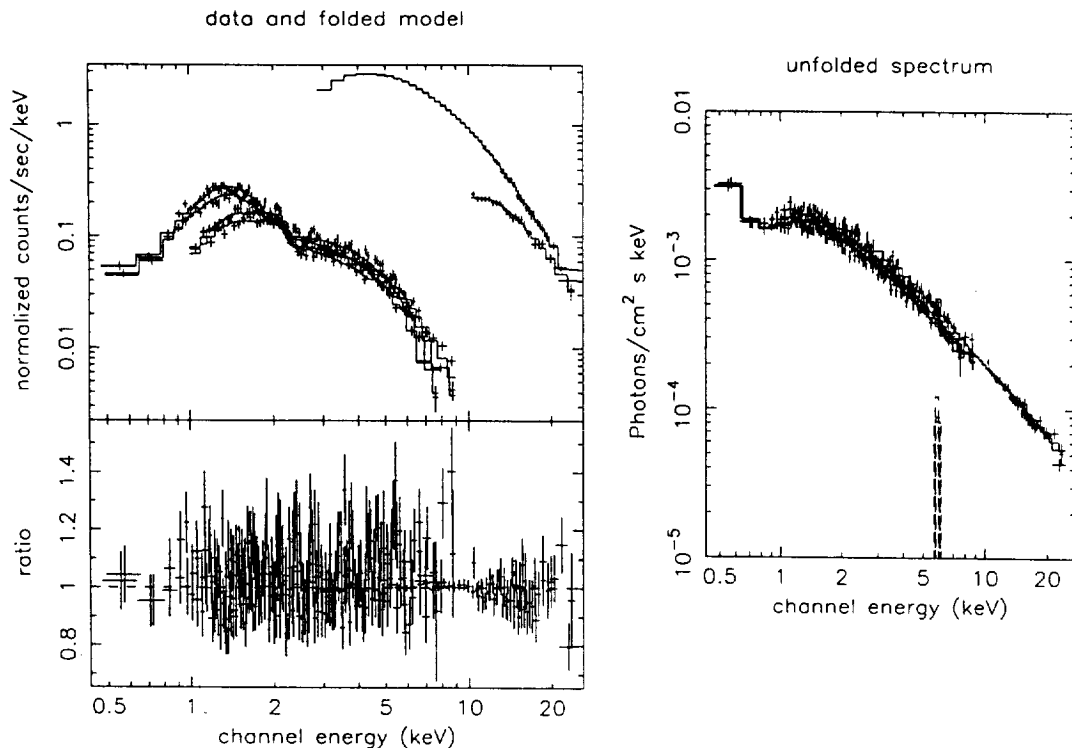


Figure 2: Results from spectral fitting of simultaneous ASCA and RXTE observation of MR 2251-178.

Columbia Astronomy Department graduate student Miranda Jackson. She has been able to produce a flux light curve as shown in Figure 1 in comparison with the *ROSAT* HRI light curve from 3C 390.3. She is currently investigating the data for systematics in the background subtraction.

Our first impression is that despite the similarity in hard X-ray luminosity, Fairall 9 appears to show much more power at high frequencies, and less power at low frequencies than 3C 390.3 did. This will be checked by performing a power spectral analysis after the systematics in the background subtraction have been quantified. It definitely does suggest that the slope of the power spectrum will be found to be distinctly flatter in Fairall 9. The character of the light curve appears distinctly different; further analysis is necessary to quantify the difference.

We are also investigating the spectral variability in Fairall 9. A softness ratio analysis shows that some spectral variability is seen, in that the spectrum becomes softer when the source is brighter. The X-ray spectrum itself shows a power law with photon index ~ 1.85 and an iron line with equivalent width ~ 220 eV.

MR 2251-178: We proposed a RXTE observation of a nearby bright radio-quiet quasar MR 2251-178 to be performed simultaneously with ASCA. The aim of the coordinate observations was to determine the strength of the quasar's reflection component, and to clarify the difference of the central regions of quasars and Seyfert 1 galaxies. In addition, we planned to constrain the iron abundance of the reflecting matter using the strengths of the line and

the reflection component. This observation will also allow us to investigate the cause of the weakness of the iron line in quasars.

The investigation is being lead by the science PI, C. Otani. The source was fairly bright when observed ($L_{2-10\text{keV}} = 2.7 \times 10^{-11} \text{ ergs s}^{-1}$). Analysis of part of the data using the new, improved background model is shown in Figure 2. The model consists of a power law plus an iron line absorbed by a mixture of neutral and ionized absorption columns. The model residuals show that there is no evidence for a reflection component. If anything, the spectrum decreases at high energies. The iron line is weak, with equivalent width of 70 eV.

NGC 6300: The improvements in background subtraction and response were taken advantage of and the *RXTE* data from the Seyfert 2 galaxy NGC 6300 were analyzed. The paper has been accepted for publication in *ApJ* (Volume 522, September 1), and a copy of the proofs has been included in this report. The paper was also presented as a poster at the 1999 HEAD meeting held in Charlottesville, South Carolina.

Bibliography

An RXTE Observation of NGC 6300: A New Bright Compton Reflection-Dominated Seyfert 2 Galaxy

K. M. Leighly, J. P. Halpern, H. Awaki, M. Cappi, & S. Ueno, 1999, *ApJ*, in press (Volume 522, Sept 1)

An RXTE Observation of NGC 6300: A New Bright Compton-Reflection Dominated Seyfert 2 Galaxy

K. M. Leighly, J. P. Halpern, & M. Cappi 1999, HEAD 31, 5.03

Karen M. Leighly
Associate Research Scientist
Columbia Astrophysics Laboratory
Columbia University

A Rossi X-Ray Timing Explorer OBSERVATION OF NGC 6300: A NEW BRIGHT COMPTON REFLECTION-DOMINATED SEYFERT 2 GALAXY

KAREN M. LEIGHLY AND JULES P. HALPERN

Columbia Astrophysics Laboratory, Columbia University, 550 West 120th Street, New York, NY 10027; leighly@ulisse.phys.columbia.edu, jules@astro.columbia.edu

HISAMITSU AWAKI

Department of Physics, Kyoto University, Kyoto 606-8502, Japan; awaki@cr.scphys.kyoto-u.ac.jp

MASSIMO CAPPI

Istituto TeSRE/CNR, Via Gobetti 101, 40129 Bologna, Italy; mcappi@tesre.bo.cnr.it

SHIRO UENO

X-ray Astronomy Group, Department of Physics and Astronomy, University of Leicester, University Road, Leicester, LE1 7RH, UK; shu@star.le.ac.uk

AND

JOACHIM SIEBERT

Max-Planck-Institut für extraterrestrische Physik, Postfach 1603, 85740 Garching, Germany; jos@mpe.mpg.de

Received 1999 March 26; accepted 1999 April 8

ABSTRACT

Scanning and pointed *Rossi X-Ray Timing Explorer* (*RXTE*) observations of the nearby Seyfert 2 galaxy NGC 6300 reveal that it is a source of hard X-ray continuum and large equivalent-width Fe K α emission. These properties are characteristic of Compton reflection-dominated Seyfert 2 galaxies. The continuum can be modeled as Compton reflection; subsolar iron abundance is required, and a high inclination is preferred. However, the poor energy resolution of *RXTE* means that this description is not unique, and the continuum can also be modeled using a “dual absorber,” i.e., a sum of absorbed power laws. Observations with higher energy resolution detectors will cleanly discriminate between these two models. Optical observations support the Compton reflection-dominated interpretation as $L_X/L_{\text{[O III]}}$ is low. NGC 6300 is notable because with $F_{2-10} \approx 6.4 \times 10^{-12}$ ergs cm $^{-2}$ s $^{-1}$, it is the second brightest such object known.

Subject headings: galaxies: active — galaxies: individual (NGC 6300) — galaxies: individual (NGC 6393) — galaxies: Seyfert — X-rays: galaxies

1. INTRODUCTION

The unified model of Seyfert galaxies proposes that orientation of a molecular torus determines the optical emission-line characteristics (e.g., Antonucci 1993). When the molecular torus lies in our line of sight, it blocks our view of the broad optical emission lines, leading to a Seyfert 2 classification. The X-ray emission of Seyfert 2 galaxies is frequently absorbed (e.g., Turner et al. 1998; Bassani et al. 1999), a result that supports this unified model. In the most extreme case, the obscuring material presents such a high column density to the observer that no X-rays are transmitted. Such objects are termed “Compton-thick” Seyfert 2 galaxies, and the only X-rays observed from them are ones that have been scattered from surrounding material. (Diffuse thermal X-rays may also contribute.) Such objects are important because they directly support unified models of Seyfert galaxies.

The scattering is thought to originate in one or both of two types of material, each of which imparts characteristic signatures on the observed X-ray spectrum (for a review, see Matt 1997). Scattering can occur in the warm optically thin gas that is thought to produce the polarized broad lines seen in some Seyfert 2 galaxies. The resulting spectrum has the same slope as the intrinsic spectrum, with superimposed emission lines from recombination. This is the process that appears to dominate in the archetypal Seyfert 2 galaxy NGC 1068 (e.g., Netzer & Turner 1997). Scattering can also occur in optically thick cool material located on the surface of the molecular torus. In this case, the process is called

Compton reflection (e.g., Lightman & White 1988), and the observed continuum spectrum is flat with superimposed K-shell fluorescence lines (e.g., Reynolds et al. 1994). Circinus can be considered the prototype of a Compton reflection-dominated Seyfert 2 galaxy (Matt et al. 1996).

Compton reflection-dominated Seyfert 2 galaxies are important because they may comprise a significant fraction of the X-ray background (Fabian et al. 1990). They were once thought to be rare (e.g., Matt 1997); however, new observations of objects selected according to their [O III] emission-line flux, a method that ideally does not discriminate against highly absorbed objects, show that they may be more common than previously thought (Maiolino et al. 1998). However, *bright* examples of this class remain rare. This is not surprising because the reflected X-rays are very much weaker than the primary continuum.

We present the results of a *Rossi X-Ray Timing Explorer* (*RXTE*) observation of the nearby (18 Mpc) Seyfert 2 galaxy NGC 6300. This object has a flat, hard X-ray spectrum and a huge equivalent-width iron line, which suggests that it is a Compton reflection-dominated Seyfert 2 galaxy. If so, it is one of the brightest members of this class known, about half as bright as the prototype, Circinus, and far brighter than other examples.

2. DATA ANALYSIS

NGC 6300 was first detected in hard X-rays during a *Ginga* maneuver (Awaki 1991). We proposed scanning and pointing observations of this galaxy using *RXTE* to

confirm the *Ginga* detection. Another Seyfert 2 galaxy, NGC 6393, was detected during a *Ginga* scan and was also investigated as part of this proposal. The data show that NGC 6393 was very faint (<0.5 counts s^{-1} in the top layer

Q3

for five proportional counter units [PCUs]). The scanning *RXTE* observation of NGC 6300 was performed on 1997 February 14–15. Four of five PCUs were on for the entire observation and analysis was confined to these detectors. A pointed observation followed on 1997 February 20, performed with all five PCUs on. The data were reduced using *Ftools* 4.1 and 4.2 and standard data selection criteria recommended for faint sources. The resulting exposure for the pointed observation was 24,896 s. NGC 6300 was detected in all three layers of the Proportional Counter Array (PCA), and the top and middle layers were used for spectral fitting. Background subtraction yielded net count rates for five PCUs of 4.4 counts s^{-1} (12.5% of the total) between 3 and 24 keV for the top layer and 0.86 counts s^{-1} (8.8% of the total) between 9 and 24 keV for the middle layer.

The current standard background model for the *RXTE* PCA is quite good; however, NGC 6300 is a relatively faint source, and therefore we attempt to estimate systematic errors associated with the background subtraction. Above 30 keV, no signal should be detected; however, we found a positive signal, which could be removed if the background normalization were increased by 1%. Below about 7 keV, no signal should be detected in the middle or bottom layers. We observed a small deficit in signal, which would be removed if the background normalization were decreased by 1%. We consider this to be evidence that the systematic error on the background subtraction is less than 1%.

The scan observation consisted of four passes over the object, with a total scan length of 6°. The scans were performed keeping the declination constant during the first two passes and the right ascension constant during the second two passes. The resulting scan profiles, when compared with the optical position, clearly indicate that NGC 6300 is the X-ray source. The field of view of the PCA is less than 2° in total width. Since the scan length was 6°, and since there are apparently no other X-ray sources in the field of view, the ends of the scan paths can be used to check the quality of the background subtraction. This was of some concern since NGC 6300 is rather near the Galactic plane ($l = 328^\circ$, $b = -14^\circ$), and thus there could be Galactic X-ray emission not accounted for in the background model. We accumulated spectra with offset from the source position greater than 1°.5. The exposure time was 1472 s. The count rate between 3 and 24 keV was -0.28 ± 0.19 counts s^{-1} , so there was no evidence for unmodeled Galactic emission. Thermal model residuals show no pattern; i.e., there is no evidence

Q4

for a 6.7 keV iron emission line from the Galactic ridge (Yamauchi & Koyama 1993). The spectrum from the pointed observation was first modeled using a power-law plus Galactic absorption set equal to 9.38×10^{20} cm $^{-2}$ (Fig. 1; Dickey & Lockman 1990). This model did not fit the data well ($\chi^2 = 609$ for 82 degrees of freedom [dof]). The photon index is very flat ($\Gamma = 0.60$), there is clear evidence for an iron emission line, and there are negative low-energy residuals. Addition of a narrow ($\sigma = 0.05$ keV) line with energy fixed at 6.4 keV improves the fit substantially ($\Delta\chi^2 = 473$), but low-energy residuals remain. Additional absorption in the galaxy rest frame improves the fit substantially ($\Delta\chi^2 = 45$). Freeing

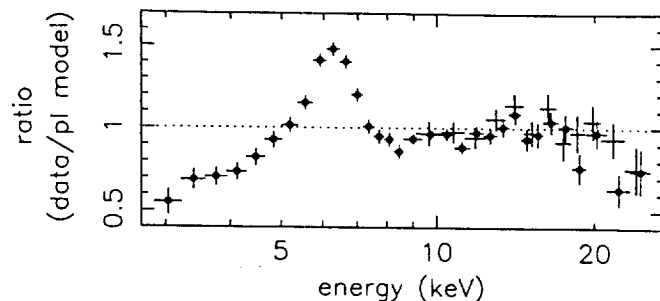


Fig. 1.—Ratio of data to a model consisting of power-law plus Galactic absorption model. The excess near 6.4 keV clearly indicates the large equivalent-width iron line. Solid points and crosses denote the top-layer and middle-layer data, respectively.

the line energy again improves the fit ($\Delta\chi^2 = 11$); the best-fit rest-frame line energy is 6.26 keV. Freeing the line width marginally improves the fit ($\Delta\chi^2 = 5$). The final fit parameters are listed in Table 1, and fit results are shown in Figure 2.

The absorbed power-law plus iron line is an acceptable model. The notable properties of the fit are a very flat photon index ($\Gamma = 0.68$) and a very large equivalent width (920 eV). Such parameters suggest that the spectrum of NGC 6300 is dominated by Compton reflection (Matt et al. 1996; Malaguti et al. 1998; Reynolds et al. 1994). We next use the *pexrav* model in XSPEC to explore this possibility. This model calculates the expected X-ray spectrum when a point source of X-rays is incident on optically thick, predominantly neutral (except hydrogen and helium) material. The parameter R measures the solid angle Ω subtended by the optically thick material: $R = \Omega/2\pi$. The model that was fitted includes a narrow iron line and a direct and reflected power law; additional absorption also appears to be necessary. The low resolution and limited bandpass provided by the *RXTE* spectrum means that not all of the model parameters could be constrained by the data; thus, the energy of the exponential cutoff was fixed at 500 keV, approximately the value that has been found in *OSSE* data from Seyfert galaxies (Zdziarski et al. 1995), and the inclination was initially fixed arbitrarily at 45°. This model provided a fairly good fit to the data ($\chi^2 = 112$ for 77 dof.). However, the best-fit value of R is very large (1450) and not well constrained. This indicates that the spectrum can be modeled using reflection alone and that there is no significant contribution from direct emission (e.g., Matt et al. 1996).

Reflection alone gives the same χ^2 as the model that includes a weak direct component, but the fit is still not completely satisfactory, and it can be improved in two ways. The first is to allow the iron abundance to vary. We set the iron abundance relative to solar in the *pexrav* model equal to the abundances of light elements and allow these parameters to vary together. The fit is improved significantly ($\Delta\chi^2 = -36$ for $\Delta\text{dof} = 1$) and gives a slightly subsolar abundance. The second is to allow the inclination to be free. The fit is not very sensitive to this parameter, as $\Delta\chi^2$ over the whole range is 9.2. The best-fit value is $\cos(\Theta) = 0.22$, corresponding to 77° from the normal. The parameters are listed in Table 1.

We investigated the choice of fixed parameters in the *pexrav* model a posteriori. Increasing the cutoff energy did not change the fit. Decreasing the cutoff to 100 keV produc-

TABLE 1
SPECTRAL FITTING RESULTS

Parameter	Value
Power-law Model	
Γ	$0.68^{+0.09,+0.16}_{-0.09,-0.13}$
$N_{\text{H}} (10^{22} \text{ cm}^{-2})$	$5.2^{+1.5,+3.5}_{-1.7,-2.7}$
$E_{\text{Fe}} (\text{keV})$	$6.26^{+0.06,+0.02}_{-0.06,-0.02}$
$\sigma_{\text{Fe}} (\text{keV})$	$0.32^{+0.13,+0.07}_{-0.16,-0.07}$
$F_{\text{Fe}} (10^{-5} \text{ cm}^{-2} \text{ s}^{-1})$	$8.2^{+1.2,-0.4}_{-1.1,+0.5}$
$\text{EW}_{\text{Fe}} (\text{eV})$	$920^{+140,-90}_{-130,+100}$
$\chi^2/79 \text{ dof}$	$75.5^{+6.7}_{-2.2}$
Compton Reflection Model	
Γ	$1.89^{+0.08,-0.13}_{-0.09,-0.08}$
Abundance ^a	$0.61^{+0.11,+0.15}_{-0.11,-0.15}$
$\cos(\Theta)$	$0.22^{+0.16,-0.04}_{-0.22,-0.02}$
$E_{\text{Fe}} (\text{keV})$	$6.29^{+0.09,-0.02}_{-0.08,-0.02}$
$\sigma_{\text{Fe}} (\text{keV})$	$0.22^{+0.20,+0.06}_{-0.22,-0.13}$
$F_{\text{Fe}} (10^{-5} \text{ cm}^{-2} \text{ s}^{-1})$	$4.7^{+1.2,+1.2}_{-1.0,-1.2}$
$\text{EW}_{\text{Fe}} (\text{eV})$	$470^{+120,+200}_{-100,-150}$
$\chi^2/77 \text{ dof}$	$70.3^{+1.6}_{-9.2}$
Dual Absorber Model	
Γ	$1.71^{+0.21,+0.27}_{-0.19,-0.21}$
$N_{\text{H}}(\text{thin}) (10^{22} \text{ cm}^{-2})$	$7.7^{+4.0,+2.0}_{-5.2,-1.4}$
$N_{\text{H}}(\text{thick}) (10^{22} \text{ cm}^{-2})$	$58^{+23,+5}_{-22,-2}$
$A_{\text{thick}}/A_{\text{thin}}^b$	$1.9^{+1.4,+1.0}_{-0.9,-0.7}$
$E_{\text{Fe}} (\text{keV})$	$6.26^{+0.09,-0.005}_{-0.12,-0.002}$
$\sigma_{\text{Fe}} (\text{keV})$	$0.23^{+0.25,-0.05}_{-0.23,-0.04}$
$F_{\text{Fe}} (10^{-5} \text{ cm}^{-2} \text{ s}^{-1})$	$3.2^{+1.4,-0.7}_{-1.5,-0.8}$
$\text{EW}_{\text{Fe}} (\text{eV})$	$470^{+210,-60}_{-220,+50}$
$\chi^2/79 \text{ dof}$	$67.6^{+2.4}_{-1.2}$

NOTE.—Two kinds of errors are given for each parameter value. The first one is the statistical error that represents 90% confidence for one parameter of interest ($\Delta\chi^2 = 2.71$). The second one is an estimate of the systematic error obtained by changing the normalization of the background. The results of background under- and oversubtraction by 1% are given in the sub- and superscript, respectively.

^a Fraction of solar abundance in iron and light elements.

^b Ratio of power-law normalizations.

ed small differences in the parameters; namely, the photon index was smaller, the abundance was higher, and the line flux was lower, but the differences are within the statistical errors of the adopted model. We also investigated the situation when the iron abundance was allowed to vary, but the abundances of lighter metals were maintained at the solar value. A significantly larger photon index by $\Delta\Gamma \approx 0.15$ was required because of the decreased reflectivity in soft X-rays. We also investigated the effect of a 1% systematic error in the background normalization, and the results are listed in Table 1. This resulted in the largest change in the fit parameters, but the resulting estimated systematic errors are in the worst case less than a factor of 2 larger than the statistical errors.

Because of the low-energy resolution of the *RXTE* spectra, other models can be found that fit equally well. It is possible to describe the spectra using a sum of absorbed power laws (the “dual absorber” model; e.g., Weaver et al. 1994). Specifically, the model consisted of two power laws, both absorbed by a moderate column and one absorbed by a heavy column. The resulting photon index was very flat

($\Gamma = 1.15$) and is therefore deemed unphysical. However, including reflection with $R = 1$ in the dual absorber model gave an insignificant improvement in fit ($\Delta\chi^2 = -0.6$) but a more plausible photon index ($\Gamma = 1.7$). The fit parameters are given in Table 1. It is notable that the spectra cannot be described using a highly absorbed transmitted component and an unabsorbed Compton reflection-dominated component, as has been found to be appropriate for Mrk 3 (Cappi et al. 1999).

3. DISCUSSION

3.1. Compton Reflection Continuum Model

The X-ray continuum of NGC 6300 can be modeled as pure Compton reflection. For solar abundance, the iron line equivalent width relative to the reflection continuum is predicted to be between 1 and 2 keV, depending on inclination (Matt, Perola, & Piro 1991). When we fit a power-law continuum to the spectra, the observed equivalent width is nearly 1 keV. However, when the reflection continuum is fitted, the measured equivalent width is reduced to 470 eV. The reason for the reduction in the measured equivalent width is that the reflection continuum model includes a substantial iron edge. In low-resolution data, the iron line and iron edge overlap in the response-convolved spectra. Therefore, when the continuum is modeled by a power law, the iron line models both the line and the edge, so the measured equivalent width is larger than when the continuum is modeled by the reflection continuum, which includes the iron edge explicitly. This effect can be seen in Figure 2.

A significant improvement is obtained when the iron abundance in the reflection continuum model is allowed to be subsolar. The iron abundance is determined by the depth of the iron edge. Therefore, the subsolar abundance fits because the iron edge is apparently not as deep as the model predicts. The fact that the iron line has a lower equivalent width than predicted in the Compton reflection continuum model may also support subsolar abundance. Alternatively, however, the apparent subsolar abundances may at least partially be due to calibration uncertainties in the *RXTE* PCA. (The resolution of the *RXTE* PCA is under some debate; see Weaver, Krolik & Pier 1998.) The iron line and edge overlap in the response-convolved spectra. If the true energy resolution is worse than the current estimated value, then because the line is an excess and the edge is a deficit, both would be measured to be smaller than they really are.

Another source of uncertainty may come from the models themselves, which depend strongly on the geometry of the illuminating and reprocessing material. Models generally assume a point source of X-rays located above a disk and illuminating it with high covering fraction. Such an ideal case may not be attained in nature.

3.2. Dual Absorber Continuum Model

The dual absorber model can also describe the spectra. That such a fit is successful is not surprising, as any flat continuum can be modeled as a sum of absorbed power laws (e.g., the X-ray background).

The iron line equivalent width for the dual absorber model is similar to that found for the Compton reflection model and smaller than that found for the power-law model. The reason for the difference is that, like the Compton reflection continuum model, the dual absorber model explicitly includes an iron edge. A plausible origin for

Q10

Q6

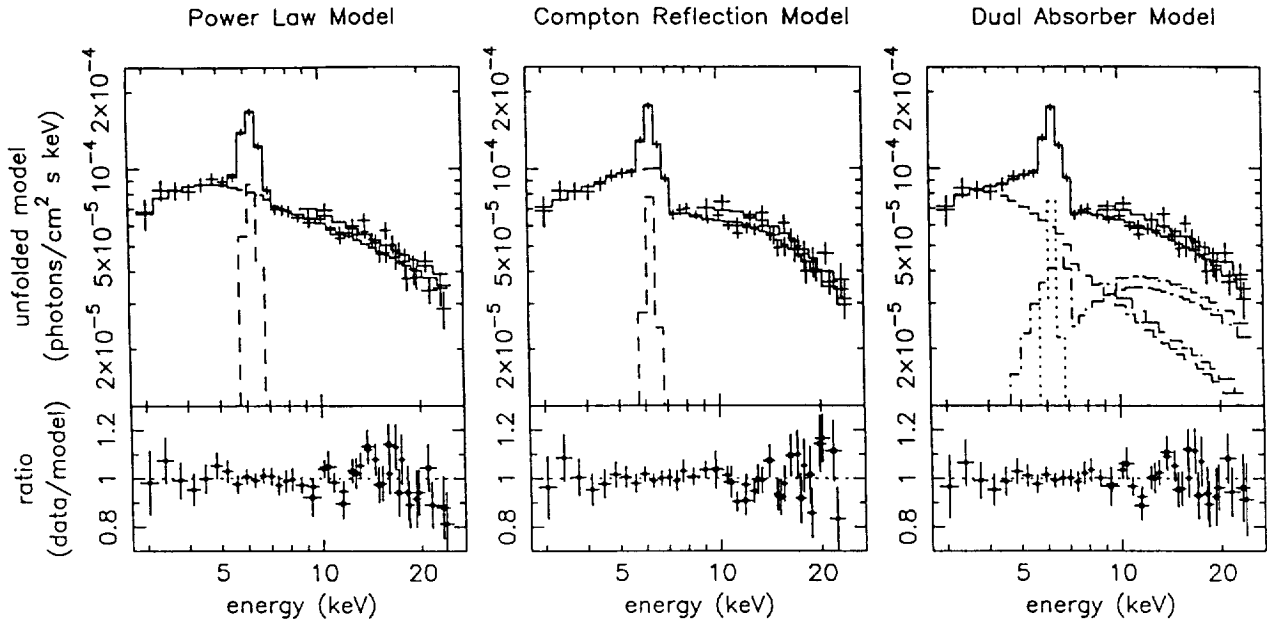


FIG. 2.—Unfolded spectra and ratio of data to model for the three models considered (see Table 1).

the iron line in the dual absorber model is in the absorbing material itself. However, the iron line equivalent width appears to be too large to have been produced in the absorbing material. We investigate this possibility by comparing the observed iron line flux to the predicted value from a spherical shell of gas surrounding an isotropically illuminating point source (Leahy & Creighton 1993). A line flux of 2.3×10^{-5} photons $\text{cm}^{-2} \text{s}^{-1}$ is predicted for the absorption columns and covering fractions determined by the fit; this is about half of what is observed (4.7×10^{-5} photons $\text{cm}^{-2} \text{s}^{-1}$). The dual absorber model also requires a reflection component with $R = 1$, and therefore an additional iron line with equivalent width ~ 100 eV is expected from the reflection. Then the predicted flux increases to 3.3×10^{-5} photons $\text{cm}^{-2} \text{s}^{-1}$, about 70% of what is observed. The predicted line flux would be smaller if the absorbing material does not completely cover the source, a circumstance that would exacerbate the difference between predicted and observed flux. Thus, the iron line equivalent width, at least to first approximation, appears to be too large to have been produced in the absorbing material required by the dual absorber model. Therefore, either an iron overabundance is required in the dual absorber model, or the alternative model, the Compton reflection-dominated model, is favored.

Discrimination between models will come with observations using detectors with better energy resolution. If NGC 6300 is a Compton-thick Seyfert 2, then we should detect soft X-ray emission lines (e.g., Reynolds et al. 1994). The lack of any observable soft excess in the *RXTE* data may imply that there is absorption by the host galaxy (see below) or that there is little contamination from thermal X-rays or scattering from warm gas. If the latter case is true, NGC 6300 will be a particularly clean example of a Compton reflection-dominated Seyfert 2 galaxy, and the observed soft X-ray emission lines should be unambiguously attributable to fluorescence. Such proof should be easily attainable, as NGC 6300 is bright compared to known Compton reflection-dominated Seyfert 2 galaxies.

3.3. Information from Other Wave Bands

Optical observations provide some support for Compton-thick absorption in NGC 6300. Intrinsically, both hard X-rays and forbidden optical emission lines should be emitted approximately isotropically; therefore, the ratio of these quantities should be the same from object to object. However, if the absorption is Compton thick, the observed hard X-ray luminosity and therefore $L_X/L_{[\text{O III}]}$ will be significantly reduced; the ratio of the power law to reflection component 2–10 keV fluxes in the *pexrav* model is ≈ 15 . Care must be taken when applying this test, as the $[\text{O III}]$ flux must be corrected for reddening in the narrow-line region, and determination of the reddening using narrow-line Balmer decrements can be difficult. The optical spectrum of NGC 6300 is dominated by starlight (e.g., Storchi-Bergmann & Pastoriza 1989); to remove the Balmer absorption from the stars, an accurate galaxy spectrum subtraction must be done. Another complication could be narrow Balmer lines from star formation. NGC 6300 has a well-studied starburst ring (e.g., Buta 1987), but $\text{H}\alpha$ images show that the H II regions are located more than 0.5 from the nucleus, with a little diffuse emission inside of that (e.g., Evans et al. 1996). High-quality long-slit spectra yield $A_v \approx 2.5$ –3 from both the red continuum and the Balmer decrement (T. Storchi-Bergmann 1999, private communication). The observed 2–10 keV flux is 6.4×10^{-12} ergs $\text{cm}^{-2} \text{s}^{-1}$ (corresponding to a luminosity of 2.5×10^{41} ergs s^{-1}). Then $L_X/L_{[\text{O III}]}$ is approximately 1.1–1.9. This value is quite low and comparable to those obtained from Compton-thick Seyfert 2 galaxies by Maiolino et al. (1998). In particular, Circinus has $F_X = 1.4 \times 10^{-11}$ ergs $\text{cm}^{-2} \text{s}^{-1}$ (Matt et al. 1999) and reddening-corrected $F_{[\text{O III}]} = 1.95 \times 10^{-11}$ ($A_v = 5.2 \pm 0.4$; Oliva et al. 1994), yielding $L_X/L_{[\text{O III}]} = 0.7$. For comparison, a reddening-corrected sample of Seyfert 1 galaxies taken from Mulchaey et al. 1994 has a mean ratio of 14.8 (1 σ range 6.4–33.9). In contrast, the intrinsic luminosity (i.e., corrected for absorption) for the dual absorber model is 6.9×10^{41}

ergs s⁻¹, implying that $L_X/L_{\text{[O III]}} \approx 3.0\text{--}5.2$.

It is notable also that NGC 6300 shows the reddest continuum toward the nucleus in a sample of objects studied with long slit spectroscopy (Cid Fernandes, Storchi-Bergmann, & Schmitt 1998). Furthermore, there seems to be a correlation between the presence of a bar in the host galaxy and the presence of a Compton-thick Seyfert 2 nucleus (Maiolino, Risaliti, & Salvati 1999); NGC 6300 has a bar (e.g., Buta 1987).

3.4. Consistency with Einstein IPC Observation

The X-ray spectra from Seyfert 2 galaxies frequently includes a soft spectral component that may originate in scattering by warm gas or diffuse thermal X-rays. However, lack of detection in an *Einstein* IPC observation, combined with the *RXTE* observation presented here, shows that there is no evidence for such a component in NGC 6300.

In 1979 NGC 6300 was observed with the *Einstein* IPC for 990 s. It was not detected, and the 3σ upper limit to the count rate was 1.19×10^{-2} counts s⁻¹ between 0.2 and 4.0 keV (Fabbiano, Kim, & Trinchieri 1992). The Compton reflection-dominated model predicts a count rate of 1.3×10^{-2} counts s⁻¹, just the same order as the upper limit and probably consistent within the uncertainties of the model and the relative flux calibrations of the two instruments.

There may be intrinsic absorption in the system, for example, from the host galaxy. The observed optical reddening of $A_v = 2.5\text{--}3.0$ corresponds to an absorption column of $4\text{--}5 \times 10^{21}$ cm⁻², assuming a standard dust to gas ratio. Including this column in the Compton reflection-dominated model leads to a predicted IPC flux of 1.1×10^{-2} counts s⁻¹, consistent with the upper limit. Because the *RXTE* bandpass is truncated at 3 keV, it is impossible to estimate with accuracy the intrinsic absorption. For the Compton-reflection model, the 90% upper limit for one parameter of interest is 1.8×10^{22} cm⁻².

Alternatively, there may have been variability within the 18 years between the IPC and the *RXTE* observation. A probable site for the reflection is the inner wall of the molecular torus, which blocks the line of sight to the nucleus. In unified models of Seyfert galaxies, this material is located outside the broad-line region and can be 1–100 pc from the nucleus. Short-term variability is not expected; long-term variability is possible but requires a long-term trend in flux.

K. M. L. acknowledges useful discussions on the *RXTE* background with Keith Jahoda and gratefully acknowledges support by NAG-4112 (*RXTE*) and NAG5-7971 (LTSA).

REFERENCES

- Antonucci, R. 1993, *ARA&A*, 31, 473
 Awaki, H. 1991, Ph.D. thesis, Univ. Nagoya
 Bassani, L., Dadina, M., Maiolino, R., Salvati, M., Risaliti, G., Della Ceca, R., Matt, G., & Zamorani, G. 1999, *ApJS*, 121, 473
 Buta, R. 1987, *ApJS*, 64, 383
 Q9 Cappi, M., et al. 1999, *A&A*, in press
 Cid Fernandes, R., Storchi-Bergmann, T., & Schmitt, H. R. 1998, *MNRAS*, 297, 579
 Dickey, J. M., & Lockman, F. J. 1990, *ARA&A*, 28, 215
 Evans, I. N., Koratkar, A. P., Storchi-Bergmann, T., Kirkpatrick, H., Heckman, T. M., & Wilson, A. S. 1996, *ApJS*, 105, 93
 Fabian, A. C., George, I. M., Miyoshi, S., & Rees, M. J. 1990, *MNRAS*, 242, 14
 Fabbiano, G., Kim, D.-W., & Trinchieri, G. 1992, *ApJS*, 80, 531
 Leahy, D. A., & Creighton, J. 1993, *MNRAS*, 263, 314
 Lightman, A. P., & White, T. R. 1988, *ApJ*, 335, 57
 Maiolino, R., Risaliti, G., & Salvati, M. 1999, *A&A*, 341, 35
 Maiolino, R., Salvati, M., Bassani, L., Dadina, M., Della Ceca, R., Matt, G., Risaliti, G., & Zamorani, G. 1998, *A&A*, 338, 781
 Malaguti, G., et al. 1998, 331, 519
 Matt, G. 1997, in *From Micro to Mega Parsec*, ed. A. Comastri, T. Venturi, & M. Bellazzini (Firenze: Societa Astronomica Italiana), 127
 Matt, G., et al. 1996, *MNRAS*, 281, L69
 ———. 1999, *A&A*, 341, L39
 Matt, G., Perola, G. C., & Piro, L. 1991, *A&A*, 247, 25
 Mulchaey, J. S., Koratkar, A., Ward, M. J., Wilson, A. S., Whittle, M., Antonucci, R. R. J., Kinney, A. L., & Hurt, T. 1994, *ApJ*, 436, 586
 Netzer, H., & Turner, T. J. 1997, *ApJ*, 488, 694
 Oliva, E., Salvati, M., Moorwood, A. F. M., & Marconi, A. 1994, *A&A*, 288, 457
 Reynolds, C. S., Fabian, A. C., Makishima, K., Fukazawa, Y., & Tamura, T. 1994, *MNRAS*, 268, L55
 Storchi-Bergmann, T., & Pastoriza, M. G. 1989, *ApJ*, 347, 195
 Turner, T. J., George, I. M., Nandra, K., & Mushotzky, R. F. 1998, *ApJ*, 493, 91
 Weaver, K. A., Krolik, J. H., & Pier, E. A. 1998, *ApJ*, 489, 213
 Weaver, K. A., Yaqoob, T., Holt, S. S., Mushotzky, R. F., Matsuoka, M., & Yamauchi, M. 1994, *ApJ*, 436, 27
 Yamauchi, S., & Koyama, K. 1993, *ApJ*, 404, 620
 Zdziarski, A. A., Johnson, W. N., Done, C., Smith, D., McNaron-Brown, K. 1995, *ApJ*, 438, L63
- Q1 1 au: In a few places "which" has been changed to "that" to reflect ApJ style. These places will be identified: please check carefully to assure that your meaning is preserved.
 Q2 2 au: "Which" has been changed to "that."
 Q3 3 au: Are PCU and PCA (below) correct as expanded?
 Q4 4 au: Units were needed after 328 and – 14; are degrees correct?
 Q5 5 au: "Which" has been changed to "that."
 Q6 6 au: "Which" has been changed to "that."
 Q7 7 au: "Which" has been changed to "that."
 Q8 8 au: Is it okay to join these sentences?
 Q9 9 au: Is it possible to provide an update?
 Q10 10 au: "Which" has been changed to "that."